Molecular simulation of chevrons in confined smectic liquid crystals

Richard E. Webster,[1] Nigel J. Mottram,[2] and Douglas J. Cleaver[1]
[1]*Materials Research Institute, Sheffield Hallam University, Sheffield S1 1WB, United Kingdom*
[2]*Department of Mathematics, University of Strathclyde, Livingstone Tower, Glasgow G1 1XH, United Kingdom*
(Received 13 January 2003; published 26 August 2003)

Chevron structures adopted by confined smectic liquid crystals are investigated via molecular dynamics simulations of the Gay-Berne model. The chevrons are formed by quenching nematic films confined between aligning planar substrates whose easy axes have opposing azimuthal components. When the substrates are perfectly smooth, the chevron formed migrates rapidly towards one of the confining walls to yield a tilted layer structure. However, when substrate roughness is included, by introducing a small-amplitude modulation to the particle-substrate interaction well depth, a symmetric chevron is formed which remains stable over sufficiently long run times for detailed structural information, such as the relevant order parameters and director orientation, to be determined. For both smooth and rough boundaries, the smectic order parameter remains nonzero across the entire chevron, implying that layer identity is maintained across the chevron tip. Also, when the surface-stabilized chevron does eventually revert to a tilted layer structure, it does so via surface slippage, such that layer integrity is maintained throughout the chevron to tilted layer relaxation process.

DOI: 10.1103/PhysRevE.68.021706 PACS number(s): 61.30.Cz, 61.20.Ja, 68.15.+e, 42.79.Kr

I. INTRODUCTION

In the chevron structure formed by confined smectic liquid crystals (LCs), the molecular layers which traverse a cell in the more conventional bookshelf arrangement become distorted into a V shape. The chevron structure was first observed in a ferroelectric smectic-*C* LC in an x-ray diffraction study by Rieker *et al.* [1], and confirmed by a study of optical modes in a thin ferroelectric LC film [2]. Subsequently, chevron structures were also found to be formed by confined smectic-*A* LC's [3].

Due to its crucial role in the bistability of surface-stabilized ferroelectric LC devices, the chevron structure has been the focus of several theoretical and experimental studies. These have concluded that chevrons form due to the mismatch which develops between bulk and surface layer periodicities because of their very different temperature dependencies [4]. The registry between smectic layers and the adsorbing substrate is thought to be essentially frozen in, a notion supported by the periodic stress oscillations measured by Cagnon and Durand on shearing a bookshelf smectic-*A* cell [5]. Indeed, recent mesoscopic theoretical work [6] and a subsequent Monte Carlo simulation study [7] of such systems showed that concerted breaking and reforming of smectic layers takes place near the center of a cell if a bookshelf-geometry confined smectic LC is sheared. The prevalence of chevron structures over tilted layer arrangements represents further evidence that surface mobility is a crucial factor: Kralj and Sluckin have argued, using Landau–de Gennes theory, that the chevron structure formed by smectic-*A* LCs is always metastable with respect to the tilted layer arrangement, but persists because the latter can only form following layer slippage at the LC-substrate interface [8]. Note, however, that a subsequent paper from the same group showed that the chevron *is* thermodynamically stable if formed by a smectic-*C* LC [9]. Shalaginov *et al.* [10,11] have also considered the presence of fluid flow during the formation of chevron structures and have estimated the time scale for molecular permeation between layers to be of the order of 10^6 s.

Continuum theory has also been used to describe the tip region of various chevron structures. The earliest treatment of this situation, due to Clark and Rieker, assumed a discontinuity in the layer tilt angle at the chevron tip [12]. Subsequent models removed this constraint, allowing, instead, quantities such as the azimuthal angle, cone angle, and layer dilatation to vary through the interface as well as the layer tilt [13,14]. More recently, these approaches have been used to treat the effects of shear on the structure and stability of the chevron [15].

Here, we present the results of parallel molecular dynamics simulations performed with the aim of determining the microscopic structure of the chevron tip. We also examine the surface conditions required to achieve the formation and stabilization of this structure. In the following section, we present the particle-surface interaction potential used for this study and list other simulation details. This is followed by a series of simulation results in Sec. III and a discussion in Sec. IV.

II. SIMULATION MODEL AND DETAILS

Throughout, the Gay-Berne (GB) potential was used for the particle-particle interactions [16], using the standard parameterization for which the phase diagram was originally determined by de Miguel *et al.* [17] ($\kappa=3$, $\kappa'=5$, $\mu=2$, $\nu=1$). This parameterization gives a length-to-breadth ratio of 3:1 and a well depth in the side-side configuration which is five times that found in the end-end configuration. We do not detail the GB model here. The particle-substrate potential used was

$$U_{S\text{-}P}(\theta_i,\phi_i,x_i,|z_i-z_0|)=\epsilon_{S\text{-}P}(\theta_i,\phi_i,x_i)\times\left[\frac{2}{15}\left(\frac{\sigma_0}{|z_i-z_0|+\sigma_0-\sigma_{S\text{-}P}(\theta_i)}\right)^9-\left(\frac{\sigma_0}{|z_i-z_0|+\sigma_0-\sigma_{S\text{-}P}(\theta_i)}\right)^3\right], \quad (1)$$

 ©2003 The American Physical Society

where the particle orientation is written in terms of the usual Euler angles, $\hat{\mathbf{u}}_i = (\cos\phi_i \sin\theta_i, \sin\phi_i \sin\theta_i, \cos\theta_i)$, the shape parameter

$$\sigma_{S\text{-}P}(\theta_i) = \frac{\sigma_0}{\sqrt{1-\chi\cos^2\theta_i}}, \tag{2}$$

$\chi = (\kappa^2 - 1)/(\kappa^2 + 1)$, and σ_0 is the particle breadth. In the absence of azimuthal coupling, this wall-particle interaction has been shown to induce tilted surface layers and, on cooling, tilted mesophases [18,19]. Additionally, the introduction of an azimuthal term, used by analogy with the experimental approach of antiparallel substrate rubbing, has been shown to yield matching pretilt orientations at a pair of opposing substrates [20].

In the simulations described in this paper, azimuthal particle-substrate coupling terms have been used again but this time with equal and *antagonistic* surface pretilts, in analogy with the parallel substrate rubbing used in the generation of pi cells [21]. Also, a spatial modulation has been applied to the particle-substrate well-depth term in order to introduce a degree of surface friction into the model; this was shown to be an effective approach in a recent paper by Binger and Hanna [22]. Thus, the complete well-depth anisotropy term took the form

$$\epsilon_{S\text{-}P}(\theta_i, \phi_i, x_i) = 2\epsilon_0[(1-\chi'\cos^2\psi_i)^\mu + \chi''(1-\cos^2\theta_i) \times \cos^2\phi_i + A(1+\sin kx_i)], \tag{3}$$

where ϵ_0 scales the well depth, $\chi' = (\kappa'^{1/\mu} - 1)/(\kappa'^{1/\mu} + 1)$, $\chi'' = 0.2$, and $\cos\psi_i = \hat{\mathbf{u}}_i \cdot \hat{\mathbf{p}}_{\text{surf}}$ is the component of $\hat{\mathbf{u}}_i$ along the surface bias vector $\hat{\mathbf{p}}_{\text{surf}}$. This approach was adopted to enable the surface pretilt to discriminate between the $+x$ and $-x$ directions: $\hat{\mathbf{p}}_{\text{surf}}$ was set to $(\pm\sin\delta, 0, \cos\delta)$ for the upper and lower substrates, respectively, with $\delta = 5°$. Note that this biasing term did not have a significant effect on the pretilt angle adopted by the surface layers; rather it broke the tilt-angle symmetry along the azimuthal easy axis. Well-depth modulation amplitudes of $A = 0.0$, $A = 0.2$, and $A = 0.5$ were used, all with $k = 32\pi/L_x$, where L_x was the length of the simulation box in the x direction. L_x and L_y were both set to $16\sigma_0$, giving a wavelength of σ_0 for each oscillation. This wavelength corresponds to the particle width rather than to the smectic layer spacing as was used in the surface energy modulation term of Ul-Islam *et al.* [14]. The shorter wavelength modulation was selected here so as not to totally inhibit at-substrate molecular slip.

Simulations were performed using the replicated-data parallel molecular dynamics code GBMESO [23] on a system of $N = 3520$ particles in the constant *NVT* ensemble. Periodic boundary conditions were imposed in the x and y directions. All simulations were performed at a number density of $0.33\sigma_0^{-3}$, giving a substrate separation L_z of $41.66\sigma_0$. Except where explicitly stated, in what follows we have employed a system of reduced units with the particle mass, breadth σ_0, and well depth ϵ_0 being set to unity. The moment of inertia orthogonal to the particle long axis was also set to 1 and the reduced time step used was $\delta t = 0.0015$. No cutoff was used for the substrate-particle interaction so that each Gay-Berne particle experienced two such interactions throughout each simulation.

The method used here to attempt to generate a chevron structure employs two surfaces to impose equal and opposite tilts on the smectic layers formed in each half of the simulation box. A slow cooling of the system into the smectic phase was judged inappropriate since the GB model has very little temperature dependence in its smectic layer spacing. Rather, the method used to induce the system to form a chevron was to quench it into the smectic phase from a point close to the nematic-smectic transition line, the expectation being that tilted layers seeded at each surface would grow and meet in the middle to form a chevron tip. The conditions for the simulation were chosen, from the phase diagram for this parameterization [17], to be a system quenched from $T = 0.95$ to $T = 0.85$.

III. RESULTS

A. Analysis

In order to extract useful mesoscopic and macroscopic variables from the numerical simulation, we have calculated block average profiles for which the computational box was divided into 120 slices parallel to the substrates. Observables were calculated separately for each slice in each saved configuration and were then averaged over the configurations to find the mean and error values for each slice.

To examine the order present in the structures formed during the simulations, the orientational order parameter S and the translational order parameter S_k were used. The parameter S and the director $\mathbf{n}$ were taken to be the largest eigenvalue and associated normalized eigenvector, respectively, of the ordering matrix $Q_{ab} = (1/2N)\Sigma_i(3u_{ai}u_{bi} - \delta_{ab})$, where δ is the Kronecker delta function. The parameter S_k corresponds to the amplitude of the smectic layer density wave and is the important order parameter during the nematic to smectic phase transition. In simulation, it can be found using

$$S_k(\mathbf{k}) = \left\langle \frac{1}{N}\left\{ \left(\sum_{i=1}^{N} \cos(\mathbf{k}\cdot\mathbf{r}_i) \right)^2 + \left(\sum_{i=1}^{N} \sin(\mathbf{k}\cdot\mathbf{r}_i) \right)^2 \right\}^{1/2} \right\rangle, \tag{4}$$

where $\mathbf{k}$ is a reciprocal lattice vector and $\mathbf{r}_i$ is the position vector of particle i. To define $\mathbf{k}$, both the smectic layer spacing and the director $\mathbf{n}$ are needed. These were determined by maximizing S_k with respect to the layer spacing by a method similar to that used in Ref. [24]. To do this, first a suitable part of a run, where stable smectic layers had formed, was selected. For each saved configuration in that part of the run, the director of the smectic region was found and then used to calculate S_k for a range of trial layer spacings from $2.5\sigma_0$ to $2.6\sigma_0$ in steps of 0.001. The layer spacing for each configuration was taken as that which maximized S_k. These values were then averaged over the selected part of the run to give the final layer spacing. Finally, this layer spacing was used,

together with the local director in each slice, to calculate S_k profiles of the system at all points in the run.

The orientational profiles are described using the commonly used director tilt angle θ, measured relative to the xy plane. We have also monitored, but do not show (for reasons of space), profiles of the director azimuthal angle ϕ, measured in the xy plane relative to the positive x axis. In smectic systems, the director tilt angle is closely related to the layer tilt angle away from the substrate normal. The position of the chevron tip was taken to be the z value of the center of the slice in which, starting at the lower surface and checking each slice in turn, the tilt angle first passed from a positive to negative value.

B. Quenching

An initial configuration was created in the nematic phase by filling the simulation box with randomly placed particles and then using a Monte Carlo method to minimize the particle overlaps [25]. The initial temperature was set to $T=1.2$ by choosing random velocities from a Maxwell-Boltzmann distribution. An initial run was performed in the constant NVE ensemble to thermalize the system, after which the system was cooled in the constant NVT ensemble from $T=1.2$ to $T=0.95$ in decrements of 0.05. Each of these runs comprised 210000 time steps and took ≈ 6 h on 32 nodes of the Edinburgh Cray T3E. The $T=0.95$ system was then equilibrated for a further 630 000 steps to give the configuration shown in Fig. 1. The desired equal and opposite surface pretilts are clearly apparent in this snapshot. The tilt angle profile $\theta(z)$ for this configuration (Fig. 2, $t=0$) also shows some chevronlike character: rather than a linear $\theta(z)$ profile, it has surface regions whose tilts are influenced by the surface pretilt, and a central region where the tilt changes more quickly. The corresponding order profiles (Figs. 3 and 4, $t=0$) show uniformly high orientational order and weak positional order across the whole box.

1. Quenching on smooth substrates

The first attempt at forming a chevron structure was made by quenching the system shown in Fig. 1 from $T=0.95$ to 0.85 with a smooth wall potential (i.e., $A=0.0$). The resultant evolution of the tilt angle profile (Fig. 2) shows that at short times, this system formed two domains of approximately equal and opposite tilt, with a relatively sharp interface between them. The corresponding order profiles (Figs. 3 and 4) show rapid onset of orientational and positional order in both domains. At much longer times, however (Figs. 2–4 at $t=10^6$ time steps), a single tilted smectic domain exists in the whole region. A snapshot of this tilted layer structure is shown in Fig. 5.

The time-resolved position of the chevron tip on quenching is shown for the entirety of this run in Fig. 6. This shows that the tip position underwent a slow drift towards the lower surface for the first 0.5×10^6 time steps of the quench, after which it experienced three sharp jumps (at $t\simeq0.5\times10^6$, 0.55×10^6, and 0.65×10^6). Closer examination of Figs. 3 and 4 shows that, throughout the quench, the smaller, lower domain (in other words that with lower z values) had slightly less orientational and positional order than the upper domain. The movement of the tip towards the lower surface appears, therefore, to have been driven by the growth of the more ordered upper domain at the expense of the less ordered lower domain.

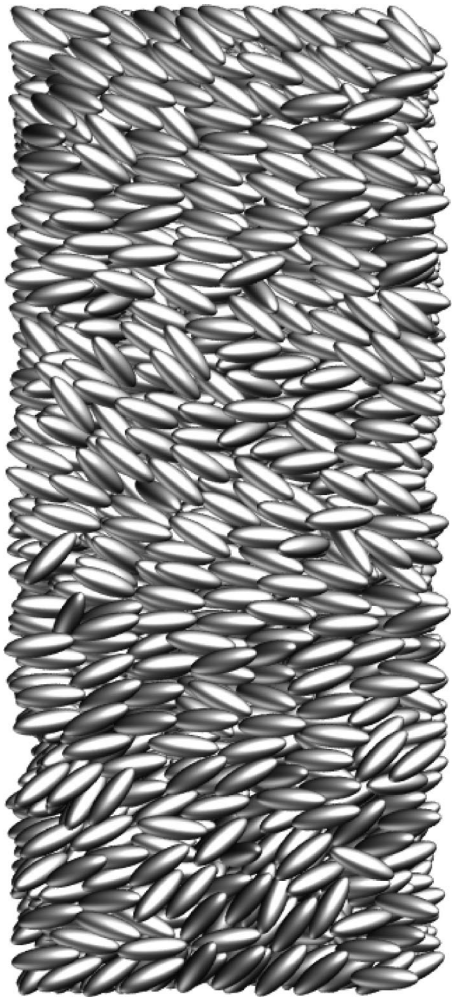

FIG. 1. Snapshot of the confined nematic system at $T=0.95$, close to the nematic-smectic transition. The lower surface is at the bottom of the picture.

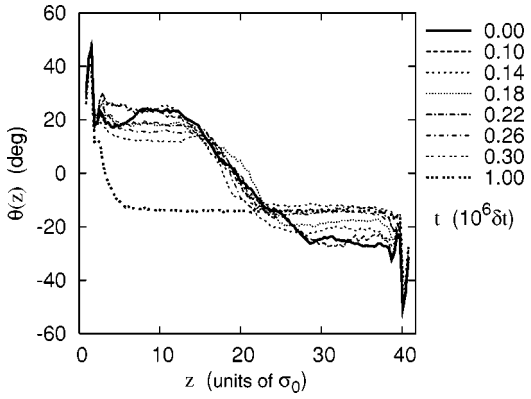

FIG. 2. Time-resolved tilt profiles for the smooth surface system quenched at $t=0$.

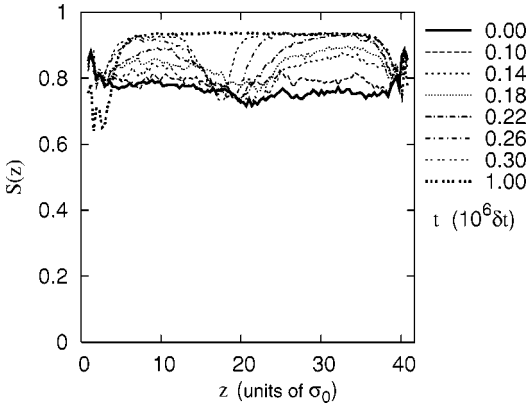

FIG. 3. Time-resolved orientational order profiles for the smooth surface system quenched at $t=0$.

2. Quenching on rough substrates

In an attempt to stabilize the chevronlike structure formed in the early stages of the smooth substrate quench, the process was repeated with rough substrates. These were created by setting the well-depth modulation parameter $A=0.5$. The rough substrates were imposed on a $T=0.95$ smooth-substrate configuration which was run on for a further 0.42×10^6 steps of equilibration prior to being quenched to $T=0.85$.

This second quench resulted in the formation of a bookshelf structure. The evolution of the tilt angle profiles (Fig. 7) indicates that, while the initial tilt profile was similar to that of the previous case, on quenching, a single domain of zero tilt was formed. The corresponding order profiles (Figs. 8 and 9) show that the order developed in a single, central region rather than the bimodal ordering mechanism seen in the smooth-substrate quench. This system, therefore, developed through the formation of a single bulk-region smectic domain which subsequently grew out towards the two substrates. A snapshot of the structure formed 0.84×10^6 time steps after the quench is shown in Fig. 10. Note, here, that the particles at the lower substrate are tilted into the plane of the figure, so the symmetry of the $\theta(z)$ profile is maintained. The profiles for this configuration (Figs. 7–9) show large disordered regions at both substrates, formed to accommodate the marked tilt and twist changes apparent from the snapshot.

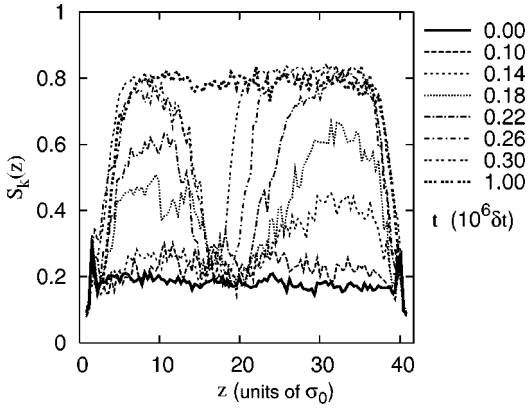

FIG. 4. Time-resolved positional order profiles for the smooth surface system quenched at $t=0$.

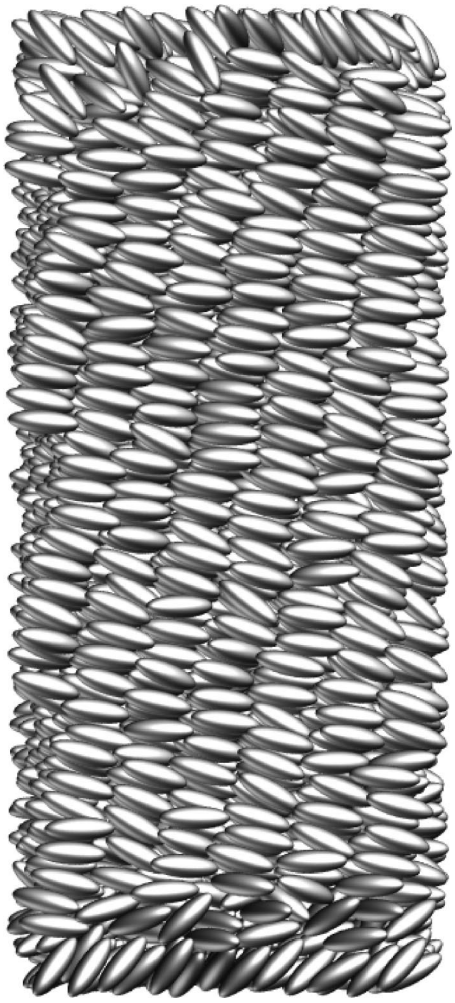

FIG. 5. Snapshot of the tilted layer structure formed by the system quenched on smooth surfaces.

3. Introducing rough substrates

Since the early stages of quenching on smooth surfaces had produced a chevronlike structure, further attempts were

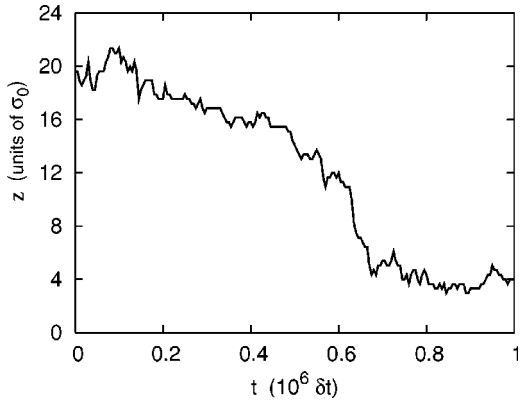

FIG. 6. Time-resolved tip position after quenching on smooth surfaces.

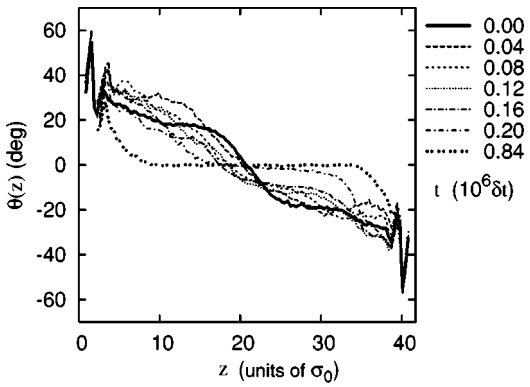

FIG. 7. Time-resolved tilt profiles for the rough surface $A=0.5$ system quenched at $t=0$.

made to stabilize this structure by introducing rough surfaces soon after quenching. To do this, various levels of substrate roughness were introduced onto the smooth surface system; Fig. 11 shows the time-resolved tip positions for a series of such simulations. To enable comparison with the systems already studied, the development of the original smooth substrate system is shown by the line marked $A=0.0$. A substrate potential term with $A=0.2$ was imposed on this at $t=0.2\times10^6$ and terms with $A=0.2$ and $A=0.4$ at $t=0.43\times10^6$. In the last two systems, the chevron tip moved towards the lower surface as with the smooth surface system, although this movement appears both to have been delayed by a small amount and to have been continuous, rather than in a series of jumps. For the first $A=0.2$ system, however, the tip steadily returned to the center of the box.

A snapshot of the resultant chevron structure is shown in Fig. 12. Block averaged profiles were created for this structure over 50 000 steps. The resultant director profiles, as shown in Fig. 13, indicate that the two domains formed with slightly different tilt angles, giving the tip a slightly asymmetrical structure. From the tilt profile, the lower portion of the tip occupies a z range of around $4\sigma_0$ whereas the upper portion occupies around $5\sigma_0$. The corresponding orientational and positional order profiles (Figs. 14 and 15) show slightly lower order in the lower half of the chevron than the upper half. Also, the low order surface region extends further

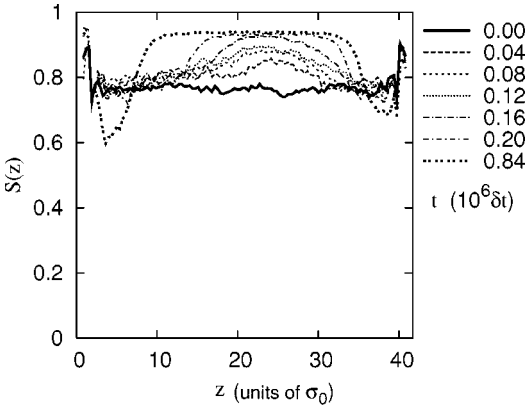

FIG. 8. Time-resolved orientational order profiles for the rough surface $A=0.5$ system quenched at $t=0$.

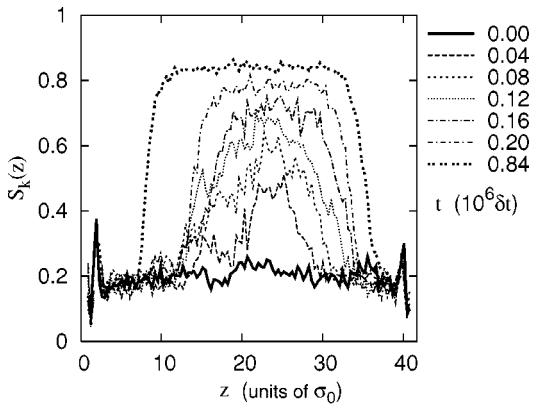

FIG. 9. Time-resolved positional order profiles for the rough surface $A=0.5$ system quenched at $t=0$.

into the bulk at the lower surface. Run averages for the smectic region in the lower half of the film give $\theta=12.4°$, $S_k=0.77$, and $S=0.93$, whereas in the upper half, the equivalent results are $\theta=-14.1°$, $S_k=0.82$, and $S=0.94$. The origin of this difference becomes apparent on seeing a snapshot of the particle positions in a single layer running from the

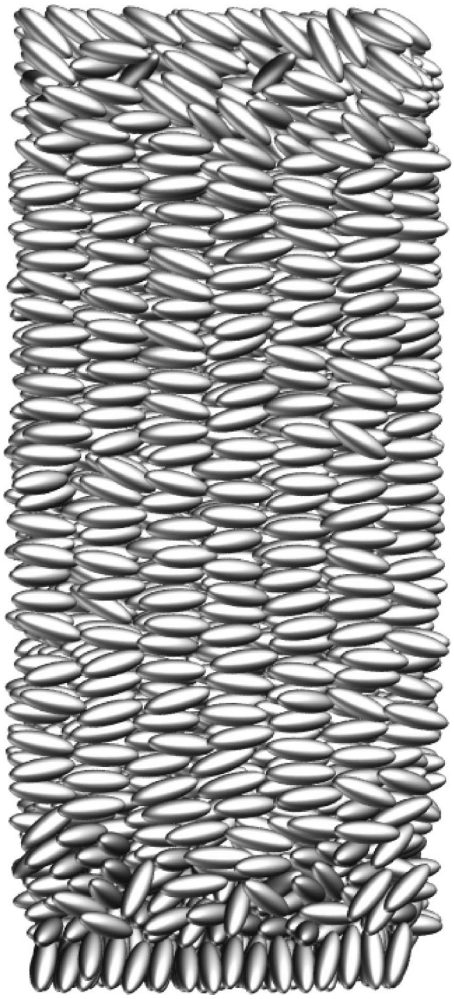

FIG. 10. Snapshot of the bookshelf structure formed on quenching the rough surface $A=0.5$ system.

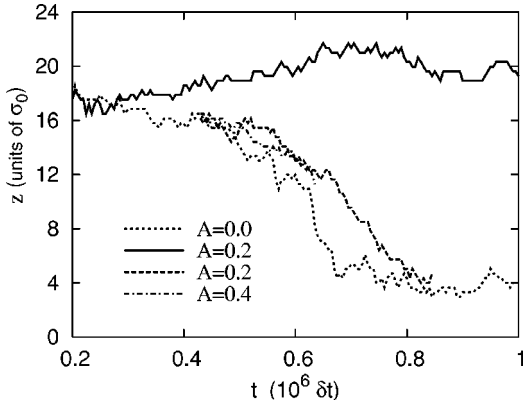

FIG. 11. Time-resolved tip position after introducing rough surfaces onto the system quenched on smooth surfaces: dotted line shows the smooth surface system which was quenched at time $t=0$ in Fig. 6, solid line shows the system with rough surfaces $A=0.2$ introduced at time $t=0.2\times10^6\,\delta t$, remaining lines show systems with rough surfaces $A=0.2$ (dash) and $A=0.4$ (dash dot) introduced at time $t=0.43\times10^6\,\delta t$.

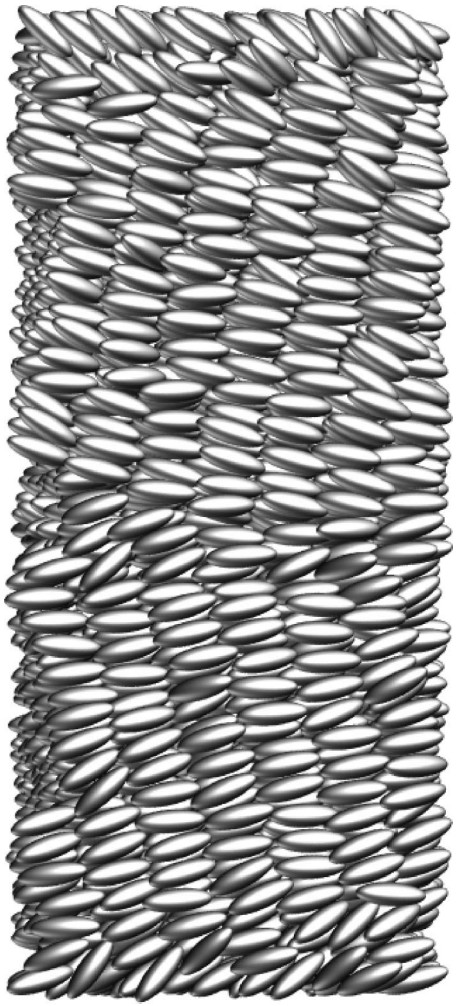

FIG. 12. Snapshot of the chevron structure formed by introducing rough surfaces $A=0.2$ onto the system quenched on smooth surfaces.

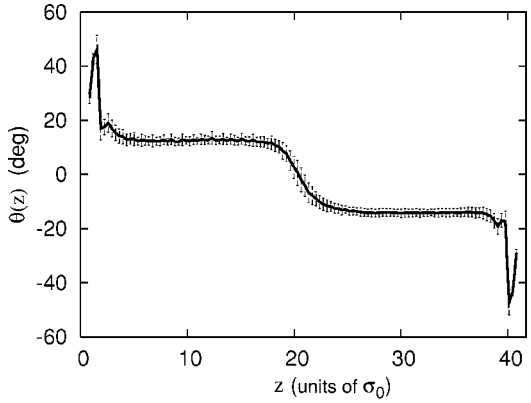

FIG. 13. Chevron structure tilt angle profile.

lower to the upper surface, as viewed along the direction of the director at the tip (Fig. 16). This shows that the orientation of the hexagonal packing of particles was different, relative to the substrate plane, for each half of the system. Since this packing geometry will certainly have influenced the coupling of the smectic layers to each surface, it seems reasonable to ascribe the asymmetries noted above to this cause. Before moving on to consider the stability of this chevron structure, we note, importantly, that Figs. 13–15 show the tip region to be associated with reductions in, but *not* vanishing of, positional and orientational order.

C. Relaxation to tilted layer structure

While the introduction of rough substrates stabilized the chevron structure over sufficiently long run times for detailed structural information to be determined, extended runs revealed that, ultimately, the chevron always relaxed to a tilted layer structure. The $A=0.2$ line in Fig. 17 shows the evolution of the chevron tip position observed during the relaxation of the chevron structure described in the preceding Subsection. The beginning of this plot overlaps the end of Fig. 11. The relaxation from chevron to tilted layer structure can be seen to have developed via an asymmetric chevron arrangement as the tip moved towards the lower surface. The other line in this figure, denoted $A=0.5$, shows the relaxation of that system but with rougher surfaces introduced at

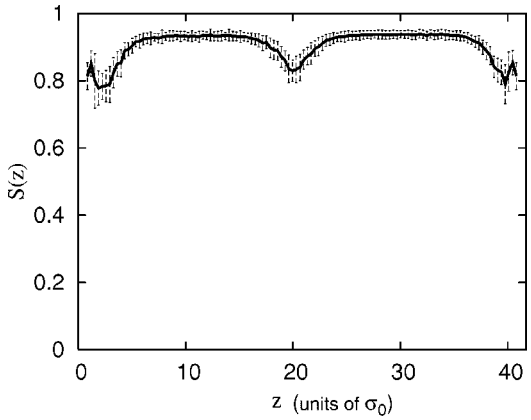

FIG. 14. Chevron structure orientational order profile.

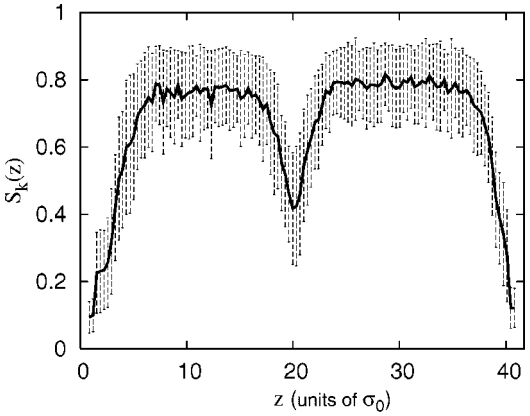

FIG. 15. Chevron structure positional order profile.

time step $t=0.41\times10^6$. This further roughening of the substrate can be seen to have delayed, but not prevented, the relaxation process. Various other modifications were made to the roughness amplitude at different points in the relaxation process, but none was found to have a significant effect on the longevity of the chevron or the mechanism of its relaxation.

The nature of the relaxation process can be determined from plots showing the histories of particles originally from a single layer of the initial chevron structure. Figure 18 shows three stages in the relaxation of the $A=0.2$ chevron system. Figure 18(a) shows, at time step $t=0.81\times10^6$, the

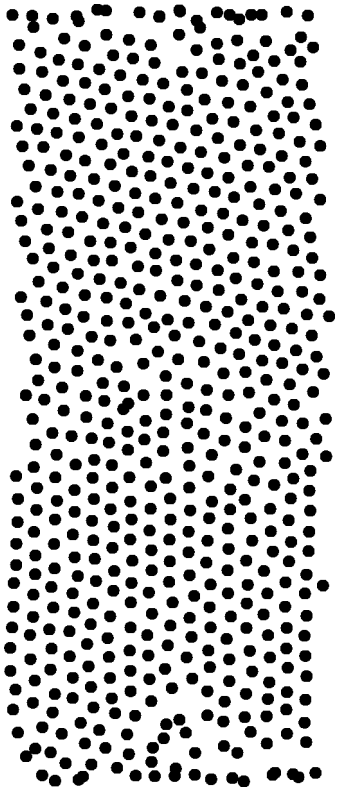

FIG. 16. Chevron structure smectic-*B* packing arrangements: positions of particles in one layer running from the lower to the upper surface, viewed along the direction of the director at the tip.

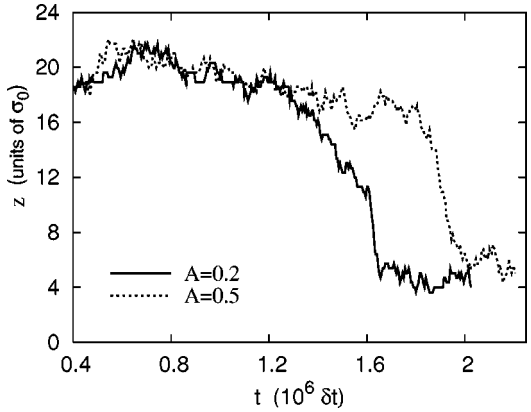

FIG. 17. Time-resolved tip position for the relaxation of the chevron structure, following from Fig. 11: solid line shows the relaxation of the $A=0.2$ surface chevron system, dashed line shows the relaxation after the introduction of rougher surfaces $A=0.5$ at $t=0.41\times10^6\delta t$.

positions of the chosen particles as black dots and the positions of the remaining particles as gray dots. Figure 18(b) shows the same system at time step $t=1.33\times10^6$, where the asymmetric chevron structure is apparent. By this stage, some diffusion of particles had occurred in the surface region and at the tip, but the layers in the lower and upper portions were still in registry. The tilted layer structure observed at time step $t=1.65\times10^6$ is shown in Fig. 18(c) and reveals that the layers maintained registry throughout the relaxation. Although not shown here, registry between lower and upper layers was found to be maintained in all of the other systems which showed relaxation from the chevron to the tilted layer structure. It is also apparent from Fig. 18 that the number of particles migrating between well-formed smectic layers was much smaller than that found in the tip and surface regions.

Since the layers maintained their registry during the relaxation process, the mechanism involved must have involved slip across the surface to allow for the relative motion of the upper and lower and upper sections of the chevron structure. This relative motion can be seen from a snapshot of a system which shows the true diffusion taking place (i.e., which has

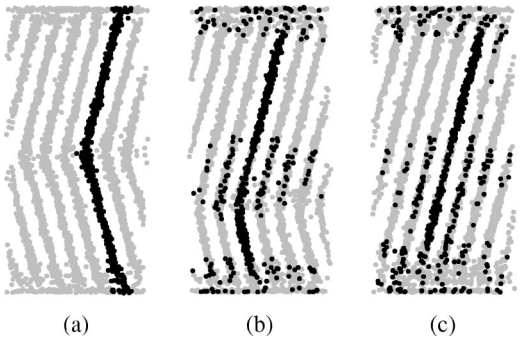

FIG. 18. Relaxation of the $A=0.2$ chevron system with black dots showing positions of particles originally in one layer and gray dots showing the remaining particles: (a) chevron structure at time step $t=0.81\times10^6\delta t$, (b) asymmetric chevron structure at time step $t=1.33\times10^6\delta t$, (c) tilted layer structure at time step $t=1.65\times10^6\delta t$.

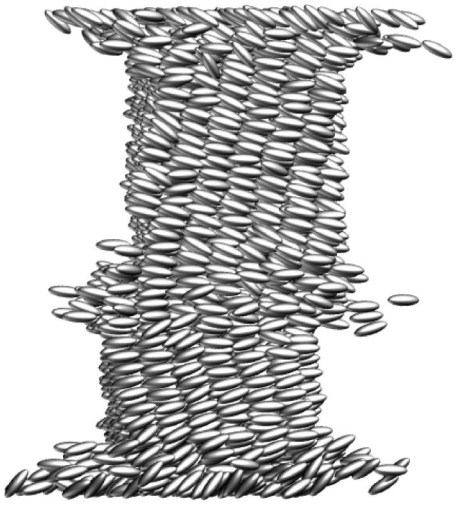

FIG. 19. Snapshot showing the true diffusion which occurred during the relaxation of the $A=0.2$ chevron system between time steps $t=1.03\times10^6\delta t$ and $t=1.24\times10^6\delta t$, created by unwrapping the effects of the periodic boundary conditions over that time period.

the effects of the periodic boundary conditions unwrapped) over a short period of the relaxation. Figure 19 shows such a snapshot of the asymmetric chevron structure. The particle positions shown are the true positions at time step $t=1.24\times10^6$, obtained by taking the particle coordinates within the simulation box at time step $t=1.03\times10^6$ as starting positions. Again, the diffusion at the surfaces and at the tip can be seen, together with an *en-masse* migration of the particles in the lower domain.

IV. DISCUSSION

In this paper, we have used molecular dynamics simulations to examine the formation, structure, and relaxation of smectic chevrons. The results demonstrate that tilted layer, chevron and bookshelf structures can all be generated by quenching a nematic system, confined by surfaces with equal and opposite pretilts, into the smectic phase; modeling of the layer-thinning mechanism thought to be responsible for chevron formation in device-scale smectic cells is not, therefore, necessary here.

The system which formed a chevron/tilted layer structure on quenching had smooth surfaces with no well-depth modulation, whereas the system which formed a bookshelf structure on quenching had rough surfaces. Due to the computational cost of these simulations, which makes assessment of reproducibility impracticable, we are unable to assert that the latter system formed a bookshelf structure solely because of the rough substrates used. In fact, we note that the initial S_k profiles of the systems at quench suggest that the differences in the structures formed may, alternatively, have arisen due to the state of each system prior to quenching. The smooth substrate system had a flat S_k profile in the bulk, whereas the rough substrate system had a slightly *n*-shaped profile. On quenching the latter, a single smectic domain grew quickly from the higher order central region, leading to the bookshelf structure—the precise role of the substrate roughness in this process is not clear. We also note that for both systems the smectic domains formed in the bulk region rather than growing out from the surfaces. This suggests that the coupling between the smectic layers and the surfaces was rather weak.

The initial chevronlike structure which formed on quenching the smooth surface system quickly relaxed to a tilted layer structure. The upper domain grew at the expense of the lower domain, presumably due to the higher orientational and positional order of the upper domain. Imposing various levels of surface roughness on this system significantly influenced the timescale of the relaxation, but did not prevent it. Rough surfaces introduced soon after the quench gave local stability to the chevron structure, causing the tip position to fluctuate about the central region. Rough surfaces introduced a short time later did not stabilize the structure but did slow the growth of the upper domain.

The profile of the stabilized chevron structure showed a small melted tip region as well as disordered regions near each surface. The effect of the periodic boundary conditions on the local tip structure is likely to have been disordering, as the director orientation at the tip would lead to a mismatch between the inherent periodicity of the smectic layers in this region and that imposed by the periodic boundaries. Therefore, the chevron tip observed in these simulations may well have been larger than that which would be formed in a system free from this constraint. The two domains which made up the chevron structure formed with slightly different values of tilt, orientational order, positional order, and orientation, relative to the surfaces, of the hexagonal packing within the layers. This again suggests relatively weak surface coupling and no direct influence of the surfaces on the internal structure within the layers.

There is an analogy to be drawn between the chevron tip formed in a confined smectic and the type of tilt grain boundary formed in regular (e.g., metal) crystals. In the presence of a nearby free surface, the mobility of such a grain boundary is governed by the relative magnitudes of the image interaction that attracts the grain boundary to the surface and the Peierls stress needed to move the underlying dislocations. In the simulations performed in this study, direct measurement of the stress profile across the chevron would have been possible, in principle, but very noisy, in practice, due to the fluctuations observed in the tip position. We can, however, estimate the extent to which the chevron-induced stress fields extended towards the confining substrates from the regions near the chevron tip in which there are marked order parameter gradients. From Fig. 14, we see that these gradients drop to 0 within $5\sigma_0$ of the chevron tip, suggesting that, prior to the final stage of rapid tip movement, the interaction between the tip and its image will have been very weak. Additionally, the relatively high molecular mobility at the chevron tip (recall Fig. 19) is inconsistent with a stress-driven dislocation hopping mechanism for the tip motion. The chevron instability observed here was not, therefore, simply a consequence of the limited film thickness accessible to our simulations.

It was found that increasing the roughness of the surfaces slowed the relaxation of the chevron to a tilted layer structure via an asymmetric chevron. This can be explained by the fact that the layers in the upper and lower domains main-

tained registry as the chevron tip moved down to the lower surface and, thus, the motion of the tip involved motion of the two domains relative to each other and to the surfaces. The low orientational order and, relative to the rest of the system, high diffusion observed at the surfaces would always be expected to result in some slippage, so it is possible that this relaxation mechanism would be relevant for any degree of pinning of the surface particles, provided that full crystallization was avoided. While we have not been able to achieve the strong layer pinning thought to be present in real confined smectics [5], our results do confirm that restricting surface mobility is key to stabilizing chevron structures.

Overall, the results presented in this paper suggest that, due to the small size of the low order surface and chevron tip regions, chevron structures can be observed in a GB system of the size simulated here. The surface roughness does appear to have influenced the stability of the chevron structure, while not fully stabilizing it. The probable mechanism for this influence is a restriction of the movement of the domains across (i.e., parallel to) the surfaces during the movement of the tip between the surfaces, the movement of the domains being necessary due to the registry maintained between the layers in the upper and lower domains.

ACKNOWLEDGMENTS

We thank C. M. Care for his comments throughout this project. This work was supported by the UK EPSRC via Grant No. GR/M16023.

[1] T.P. Rieker, N.A. Clark, G.S. Smith, D.S. Parmar, E.B. Sirota and C.R. Safinya, Phys. Rev. Lett. **59**, 2658 (1987).
[2] S.J. Elston and J.R. Sambles, Appl. Phys. Lett. **55**, 1621 (1989).
[3] See, e.g., Y. Takanishi, Y. Ouchi, H. Takezoe, and A. Fukuda, Jpn. J. Appl. Phys. **28**, L487 (1989).
[4] L. Limat and P. Prost, Liq. Cryst. **13**, 101 (1993).
[5] M. Cagnon and G. Durand, Phys. Rev. Lett. **70**, 2742 (1993).
[6] N.J. Mottram, T.J. Sluckin, S.J. Elston, and M.J. Towler, Mol. Cryst. Liq. Cryst. **347**, 423 (2000).
[7] G.R. Luckhurst, G. Saielli, and T.J. Sluckin, Phys. Rev. E **65**, 041717 (2002).
[8] S. Kralj and T.J. Sluckin, Phys. Rev. E **50**, 2940 (1994).
[9] N. Vaupotič, S. Kralj, M. Čopič, and T.J. Sluckin, Phys. Rev. E **54**, 3783 (1996).
[10] A.N. Shalaginov, L.D. Hazelwood, and T.J. Sluckin, Phys. Rev. E **58**, 7455 (1998).
[11] A.N. Shalaginov, L.D. Hazelwood, and T.J. Sluckin, Phys. Rev. E **60**, 4199 (1999).
[12] N.A. Clark and T.P. Rieker, Phys. Rev. A **37**, 1053 (1988).
[13] A. de Meyere, H. Pauwels, and E. de Ley, Liq. Cryst. **14**, 1269 (1993).
[14] N. Ul-Islam, N.J. Mottram, and S.J. Elston, Liq. Cryst. **26**, 1059 (1999).
[15] N.J. Mottram and S.J. Elston, Eur. Phys. J. B **12**, 277 (1999).
[16] J.G. Gay and B.J. Berne, J. Chem. Phys. **74**, 3316 (1981).
[17] E. de Miguel, L.F. Rull, M.K. Challam, and K.E. Gubbins, Mol. Phys. **74**, 405 (1991).
[18] Z. Zhang, A. Chakrabarti, O.G. Mouritsen, and M.J. Zuckermann, Phys. Rev. E **53**, 2461 (1996).
[19] G.D. Wall and D.J. Cleaver, Phys. Rev. E **56**, 4306 (1997).
[20] R. Latham and D.J. Cleaver, Chem. Phys. Lett. **330**, 7 (2000).
[21] P.J. Bos and K.R. Beran, Mol. Cryst. Liq. Cryst. **113**, 329 (1984).
[22] D.R. Binger and S. Hanna, Liq. Cryst. **28**, 1215 (2001).
[23] M.R. Wilson, M.P. Allen, M.A. Warren, A. Sauron, and W. Smith, J. Comput. Chem. **18**, 478 (1997).
[24] M.A. Bates and G.R. Luckhurst, J. Chem. Phys. **110**, 7087 (1999).
[25] R. E. Webster, Ph.D. thesis, Sheffield Hallam University, 2001.